Supplementary Information (SI) for Journal of Materials Chemistry A.
This journal is © The Royal Society of Chemistry 2025

Supplementary Information

Effect of π-bridge lengths in oligomerized fused-ring electron acceptor on the photovoltaic performance of organic solar cells

Mingxin Sun,[a,b,c] Jianxiao Wang,[b,c,d] Cheng Sun,*[b,c,d] Bin Tang,[a,b,c] Xiaofei Qu,*[a] Shuguang Wen,[b,c,d] and Xichang Bao*[a,b,c,d]

[a] College of Materials Science and Engineering, Qingdao University of Science and Technology, Qingdao 266042, China

[b] Key Laboratory of Photoelectric Conversion and Utilization of Solar Energy, Qingdao Institute of Bioenergy and Bioprocess Technology, Chinese Academy of Sciences, Qingdao 266101, China

[c] Laboratory of Solar Energy, Shandong Energy Institute, Qingdao 266101, China

[d] Qingdao New Energy Shandong Laboratory, Qingdao 266101, China

Keywords: Organic solar cells, Oligomer acceptors, π-bridge, Photovoltaic efficiency, Device stability

Experimental Procedures

Materials and Characterization Techniques

Donor material PM6 were purchased from Solarmer Materials Inc. Other reagents were purchased from Alfa Aesar, Sigma-Aldrich, et al., which were utilized directly unless stated otherwise.

^{1}H NMR spectra were recorded on Bruker AVANCE III 600 MHz spectrometer at 298 K. The absorption spectra were recorded using a Hitachi U-4100 UV-Vis scanning spectrophotometer. Cyclic voltammetry (CV) measurements were performed on a CHI660D electrochemical workstation, equipped with a three-electrode cell consisting of a platinum working electrode, a saturated calomel electrode (SCE) as reference electrode and a platinum wire counter electrode. CV measurements were carried out in anhydrous acetonitrile containing 0.1 mol/L Bu_4NPF_6 as a supporting electrolyte under an argon atmosphere at a scan rate of 100 mV s^{-1} assuming that the absolute energy level of Fc/Fc^+ was -4.80 eV. The formula for calculating the HOMO energy level (E_{HOMO}) and LUMO energy level (E_{LUMO}) from its initial oxidation potential φ_{ox} and initial reduction potential φ_{red} is: $E_{HOMO} = -IP = -e(\varphi_{ox} - \varphi(Fc^+/Fc) + 4.8)(eV)$, $E_{LUMO} = -EA = -e(\varphi_{red} - \varphi(Fc^+/Fc) + 4.8)(eV)$. Thin films of two acceptors were deposited from $CHCl_3$ solutions for the measurements of UV-vis absorption spectra. The thickness of films was measured using a Veeco Dektak 150 profilometer.

Contact angles are measured by the contact angle measuring instrument CSCDIC-200S. Contact angle test: The two liquid method is used to measure the contact angles. The active layers were coated onto the glass substrate. The treatment of thin films is the same as that of devices. Subsequently, During the contact angle test with the contact angle measuring instrument, H_2O and CH_2I_2 droplets contact the surface of the film and quickly disengage. By using the video recording function of the instrument, the continuous image of the drop, contact and stability of the droplets on the surface of the active layer can be obtained, so as to accurately judge the contact angle image of CH_2I_2 droplets in the active layer.

In-situ absorptions were carried out from the in-situ dynamic spectrometer DU-300, with chloroform as the solvents. Grazing incidence wide-angle X-ray scattering (GIWAXS) patterns were acquired from Shanghai Synchrotron Radiation Facility at the beam BL6B1. Transmission electron microscopy (TEM) images were obtained by using a HITACHI H-7650 electron microscope with an acceleration voltage of 100 kV. Atomic force microscopy (AFM) images were obtained using Agilent 5400 scanning probe microscope in tapping mode with MikroMasch NSC-15 AFM tips.

UV-vis spectroscopy to measure the T_g of oligomer acceptors. Test method: Once the freshly prepared thin films had dried under dynamic vacuum for an hour, their as-cast (UV–vis) spectra were acquired using a Hitachi U-4100 UV-vis spectrometer; the range of wavelengths measured was from 300 to 1100 nm with a sampling increment of 1 nm (a pristine glass slide was used as a baseline for the absorption). The glass-supported films were then immediately heated for 8 min on the surface of a hot plate in a nitrogen-atmosphere glovebox, after which they were suspended in air and allowed to cool to room temperature (TR, ~25 °C) for 3 min prior to acquiring their "annealed" spectra. Starting at TR, each film was annealed in various increments of temperature (5 °C, 10 °C, or 20 °C) depending on how far its nominal T_g was from TR. Once the annealing temperature rises to 180 °C or sufficiently surpassed the nominal T_g of the materials under investigation, the measurement was completed.

Device Fabrication and Evaluations

All the solar cells were fabricated with a conventional device structure of ITO/PEDOT:PSS/active layer/PDINN/Ag. The patterned ITO glass (sheet resistance = 15 Ω/square) was pre-cleaned in an ultrasonic bath of acetone and isopropyl alcohol and treated in an ultraviolet-ozone chamber (PREEN II-862) for 6 min. Then a thin layer (about 30 nm) of PEDOT:PSS was spin-coated onto the ITO glass at 4000 rpm and baked at 150 ℃ for 15 min. Solutions of active layers in chloroform (7.5 mg/mL for PM6) were stirred for 2.0 hrs at 50 ℃ before spin-coating on the PEDOT:PSS layer to form the active layer about 100±20 nm. The thickness of the active layer was measured using a Veeco Dektak 150 profilometer. Then PDINN (in CH_3OH, 1mg/mL) was spin-coating at 3000 rpm to form the electron transfer layer. Finally, Ag (60 nm) metal electrode was thermal evaporated under about 5×10^{-4} Pa and the device area was 0.1 cm^2 defined by shadow mask.

The current density–voltage (*J–V*) characteristics were recorded with a Keithley 2400 source measurement unit under simulated 100 mW cm^{-2} irradiation from a Newport solar simulator. The external quantum efficiencies (EQEs) were analyzed using a certified Newport incident photon conversion efficiency (IPCE) measurement system. The hole mobility and electron mobility were measured by space-charge-limited current (SCLC) method with a device configuration of ITO/PEDOT:PSS/active layer/MoO_3/Ag and ITO/ZnO/active layer/PDINO/Ag structure, respectively. The SCLC is described by the Mott–Gurney law:

$$J = 9\varepsilon\mu V^2/(8L^3)$$

where ε represents the dielectric constant of the metal, and μ is the carrier mobility, V is the voltage

drop across the device and *L* is the thickness of the active layer.

The storage stability was performed in a nitrogen filled glove box, which possesses oxygen content below 0.1 ppm, and water content below 0.1 ppm. The device was placed under dark, and the light was only turned on when measuring the *J-V* plots. Every data point was averaged from at least five independent devices.

Materials Synthesis

Synthesis of TBT

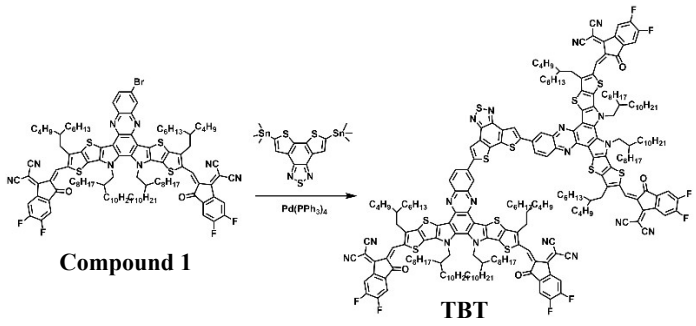

Compound 1 **TBT**

The synthesis details are listed below:

Compound 1 (250 mg, 0.13 mmol) and 5,8-bis(trimethylstannyl)dithieno[3',2':3,4;2",3":5,6]benzo[1,2-c][1,2,5]thiadiazole were added into Schlenk tube with toluene under the nitrogen atmosphere, after vacuuming and refilling with argon for three times, $Pd(PPh_3)_4$ were added to the reaction flask and continue purging with N_2 for 10 mins. The reaction was heated to 110 ℃ and stirred for another 24 h. After cooling down, the reaction mixture was participated into methanol. The solid was filtered and further purified with silica gel column chromatography to afford black solid (71% yield). ^{1}H NMR (600 MHz, Chloroform-d) δ 9.49 – 8.85 (m, 4H), 8.79 – 7.91 (m, 12H), 7.89 – 7.59 (m, 4H), 5.27 – 4.67 (m, 8H), 3.61 – 2.13 (m, 16), 1.89 – 0.99 (m, 192H), 0.93 – 0.53 (m, 48H).

Synthesis of CH-TRZ

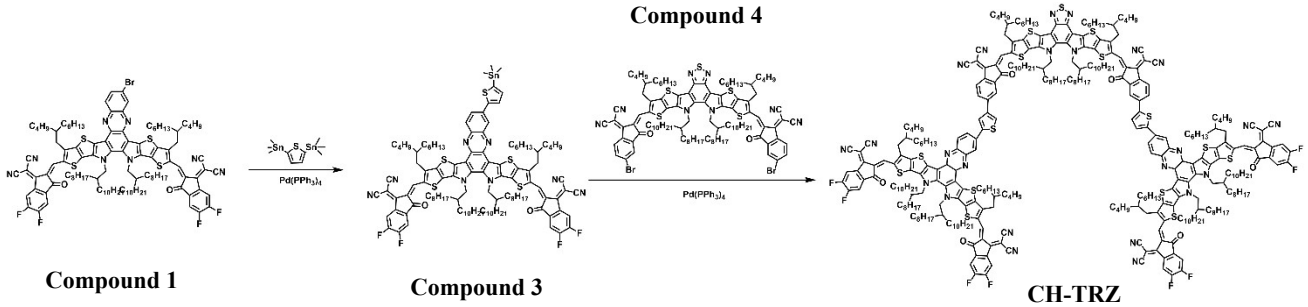

Compound 1 **Compound 3** **CH-TRZ**

The synthesis details are listed below:

Compound 1 (250 mg, 0.13 mmol), 2,5-bis(trimethylstannyl)thiophene (528 mg, 1.3 mmol), and $Pd(PPh_3)_4$ (5mg, 0.0043mmol) were combined in a 100 mL two-necked flask. Anhydrous toluene (50 mL) was added under the argon atmosphere. The mixture was reacted for 3 h at 70 °C. The crude product was precipitated in methanol and washed with methanol for three times, Compound 3 was used for next step without further purification. Compound 4 (250 mg), Compound 3 (75mg, 0.04 mmol), and $Pd(PPh_3)_4$ (5mg, 0.0043mmol) were combined in a 100 mL two-necked flask. Anhydrous toluene (50 mL) was added under the argon atmosphere. The mixture was reacted for 12 h at 110 °C. After removing residual solvents at low pressure (< 300 mbar) by a rotary evaporator, the product was purified by silica-gel column chromatography using hexane/ chloroform (1:2) as eluent to give CH-TRZ as black solid (160 mg, 72%). ^{1}H NMR (600 MHz, Chloroform-d) δ 9.17 – 8.68 (m, 6H), 8.66 – 8.48 (s, 2H), 8.46 – 8.06 (s, 8H), 8.05 – 7.59 (m, 10H), 7.59 – 7.45 (m, 2H), 7.39 – 7.28 (m, 2H), 5.47 – 4.61 (s, 12H), 3.81 – 2.58 (m, 12H), 2.45 – 2.17 (m, 12H), 1.52 – 0.97 (m, 288H), 0.96 – 0.69 (m, 72H).

Supplementary Figures

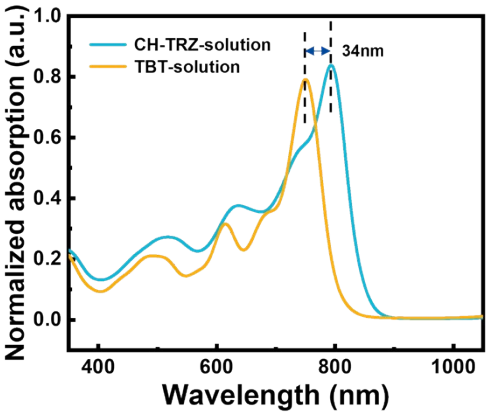

Fig. S1. Absorption spectra of the oligomers in dilute chloroform solutions, the test concentration is 1.5×10^{-6} mol/L.

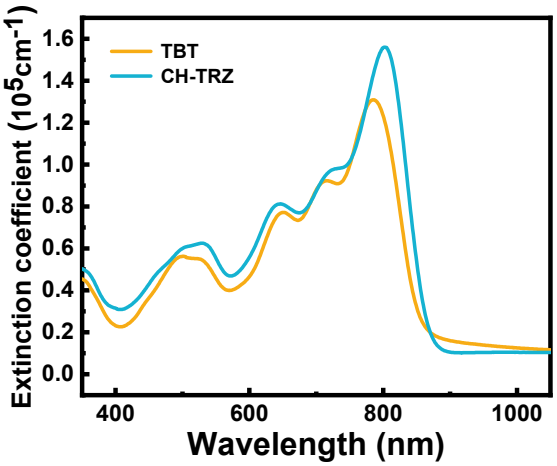

Fig. S2. Extinction coefficient spectra of TBT and CH-TRZ neat films.

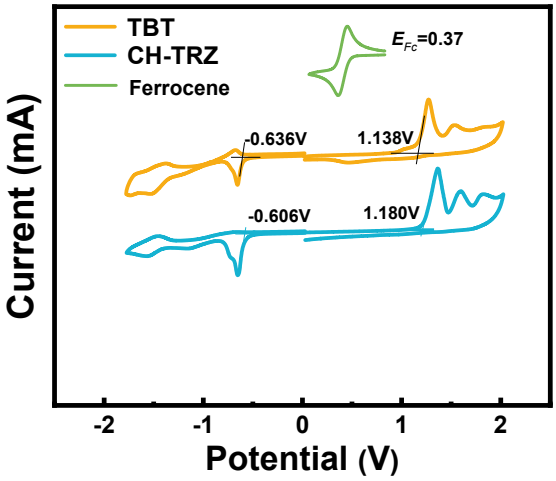

Fig. S3. The CV plots of TBT and CH-TRZ deposited on glassy carbon electrodes in 0.1 M Bu_4NPF_6-CH_3CN at a scan rate of 100 mV s^{-1}.

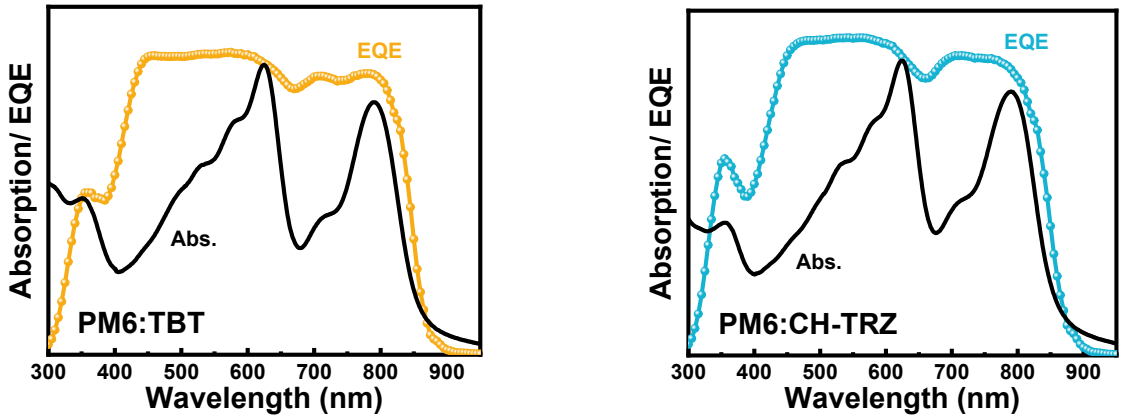

Fig. S4. The comparison of EQE profiles and blend absorption spectra.

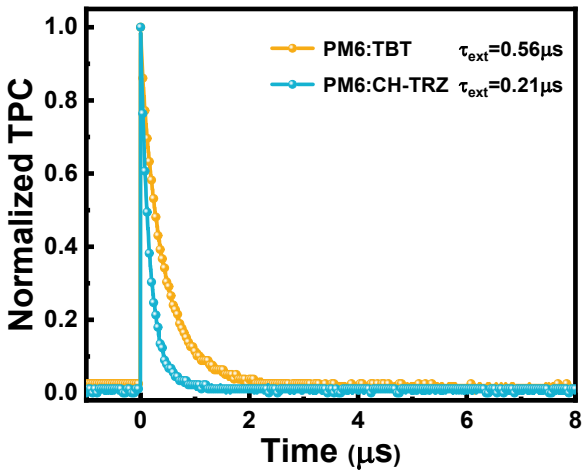

Fig. S5. Normalized TPC decays of the PM6:TBT and PM6:CH-TRZ binary solar cells.

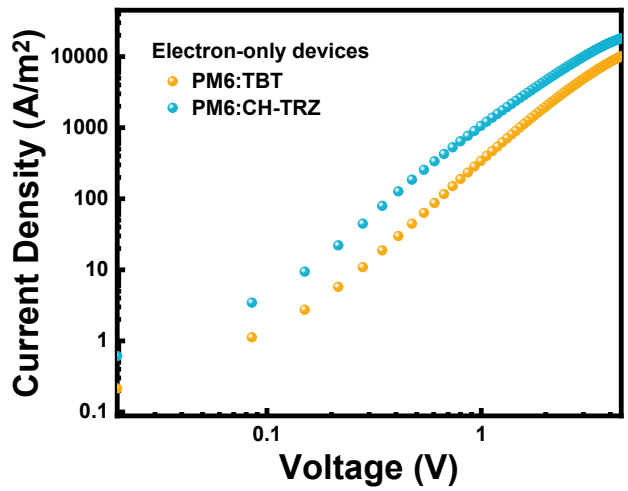

Fig. S6. SCLC curves of the electron-only devices.

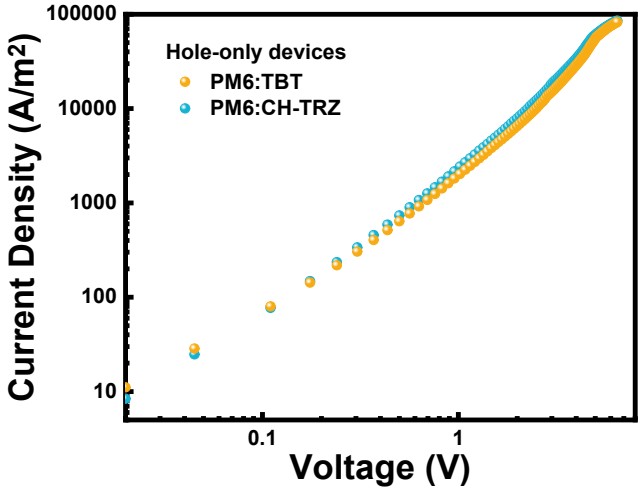

Fig. S7. SCLC curves of the Hole-only devices.

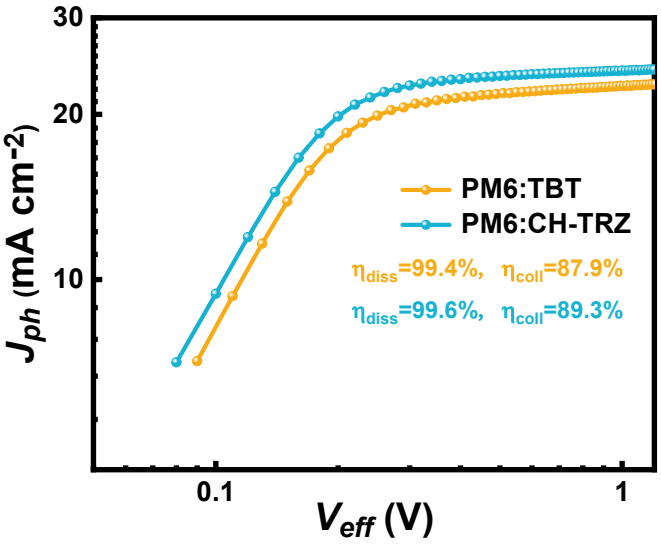

Fig. S8. J_{ph} vs V_{eff} plots.

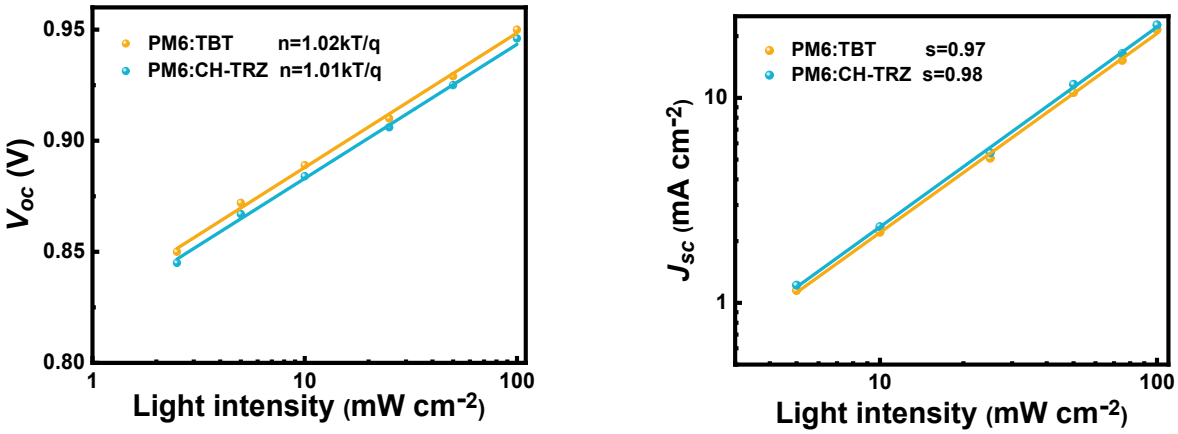

Fig. S9. (a) J_{SC} *versus* light intensity and (b) V_{OC} *versus* light intensity plots of PM6:TBT and PM6:CH-TRZ solar cells.

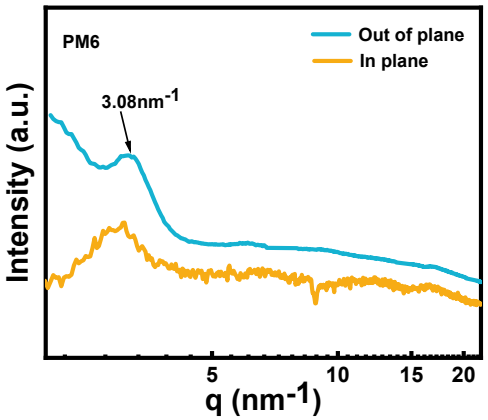

Fig. S10. Line-cut profiles of neat PM6 film from GIWAXS patterns.

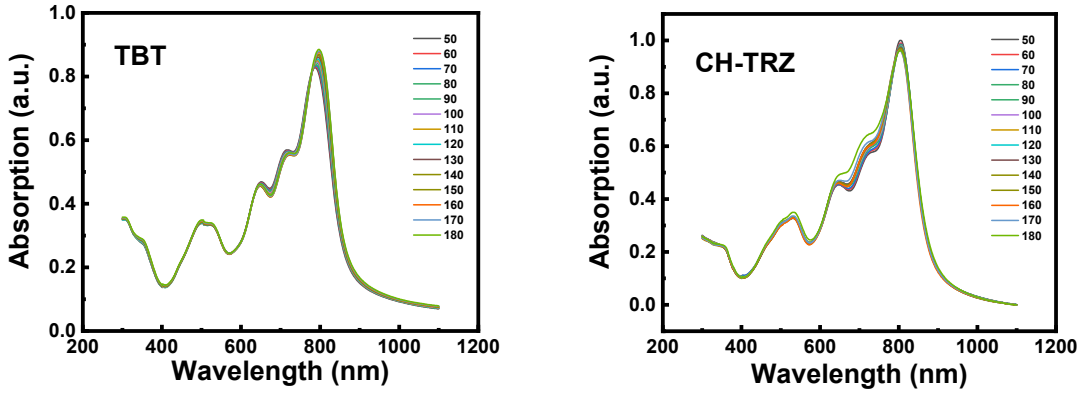

Fig. S11. Absorption spectra of TBT and CH-TRZ films as the thermal annealing temperature increases.

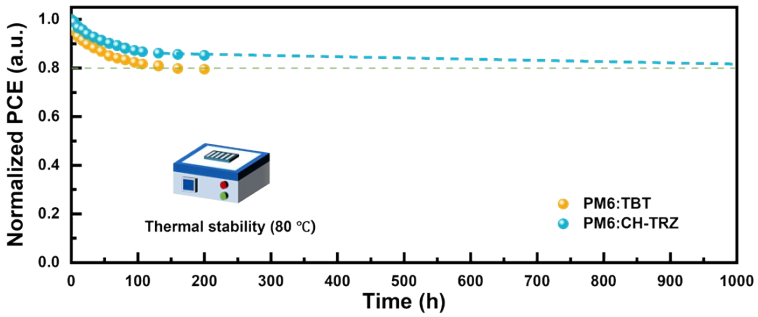

Fig. S12. Thermal stabilities under continuous heating at 80 °C.

Supplementary Tables

Table S1. Basic physical properties and frontier energy levels of TBT and CH-TRZ.

Material	λ_{max} (nm)		λ_{onset} (nm)	E_g^{opt}	LUMO	HOMO
	Solution	film	film	(eV)[a]	(eV)^{CV}	(eV)^{CV}
TBT	750	787	857	1.45	-3.79	-5.57
CH-TRZ	793	803	868	1.43	-3.82	-5.61

[a] Calculated from onset wavelength of film absorption spectra.

Table S2. The parameters of surface energies and contact angles.

Active layer	γ_s (mN m^{-1})	γ_p (mN m^{-1})	γ_d (mN m^{-1})	CA (H_2O)	CA (CH_2I_2)
PM6	37.48	1.06	36.42	107.03	51.30
TBT	39.39	0.17	39.23	98.46	44.26
CH-TRZ	38.56	0.30	38.25	100.59	46.50

Table S3. The *q* locations and π-π-stacking distances in IP and OOP directions of TBT and CH-TRZ neat films.

Film	*q* (Å^{-1})	*d* (Å)	FWHM (Å^{-1})	CCL (Å)	*q* (Å^{-1})	*d* (Å)	FWHM (Å^{-1})	CCL (Å)
	IP (100) $_{laminar}$				OOP (010) $_{\pi-\pi}$			
TBT	0.312	20.14	0.227	27.68	1.607	3.910	0.304	20.67
CH-TRZ	0.315	19.95	0.192	32.72	1.595	3.939	0.281	22.36

CCL obtained using Scherrer's equation (CCL=2π/FWHM) for the peaks in IP and OOP direction.

Table S4. Photovoltaic parameters of the PM6:TBT and PM6:CH-TRZ based OSCs at different conditions.

Active layer	CN	TA	V_{OC}	J_{SC}	FF	PCE
	v/v	℃	(V)	(mA cm^{-2})	(%)	(%)
PM6:TBT	0.5%	95	0.954	22.35	73.26	15.62
	0.7%	90	0.956	20.86	73.71	14.70
		95	**0.953**	**22.63**	**73.05**	**15.76**
		100	0.950	22.19	72.09	15.20
	1.0%	95	0.951	21.54	73.34	15.03
PM6:CH-TRZ	0.5%	95	0.946	23.53	75.00	16.69
	0.7%	90	0.952	23.43	73.76	16.46
		95	**0.948**	**23.79**	**75.62**	**17.07**
		100	0.945	23.49	74.12	16.45
	1.0%	95	0.942	23.75	75.37	16.85

Table S5. The *q* locations and π-π-stacking distances in OOP and IP directions of GIWAXS studies.

Film	*q* (Å^{-1})	*d* (Å)	FWHM (Å^{-1})	CCL (Å)	*q* (Å^{-1})	*d* (Å)	FWHM (Å^{-1})	CCL (Å)
	OOP (100) $_{laminar}$				OOP (010) $_{\pi\text{-}\pi}$			
PM6:TBT	0.308	20.40	0.076	82.67	1.664	3.776	0.232	27.08
PM6:CH-TRZ	0.308	20.40	0.075	83.78	1.651	3.805	0.229	27.44

Film	*q* (Å^{-1})	*d* (Å)	FWHM (Å^{-1})	CCL (Å)
	IP (100) $_{laminar}$			
PM6:TBT	0.293	21.44	0.099	63.47
PM6:CH-TRZ	0.299	21.01	0.098	64.11

Supplementary NMR spectra

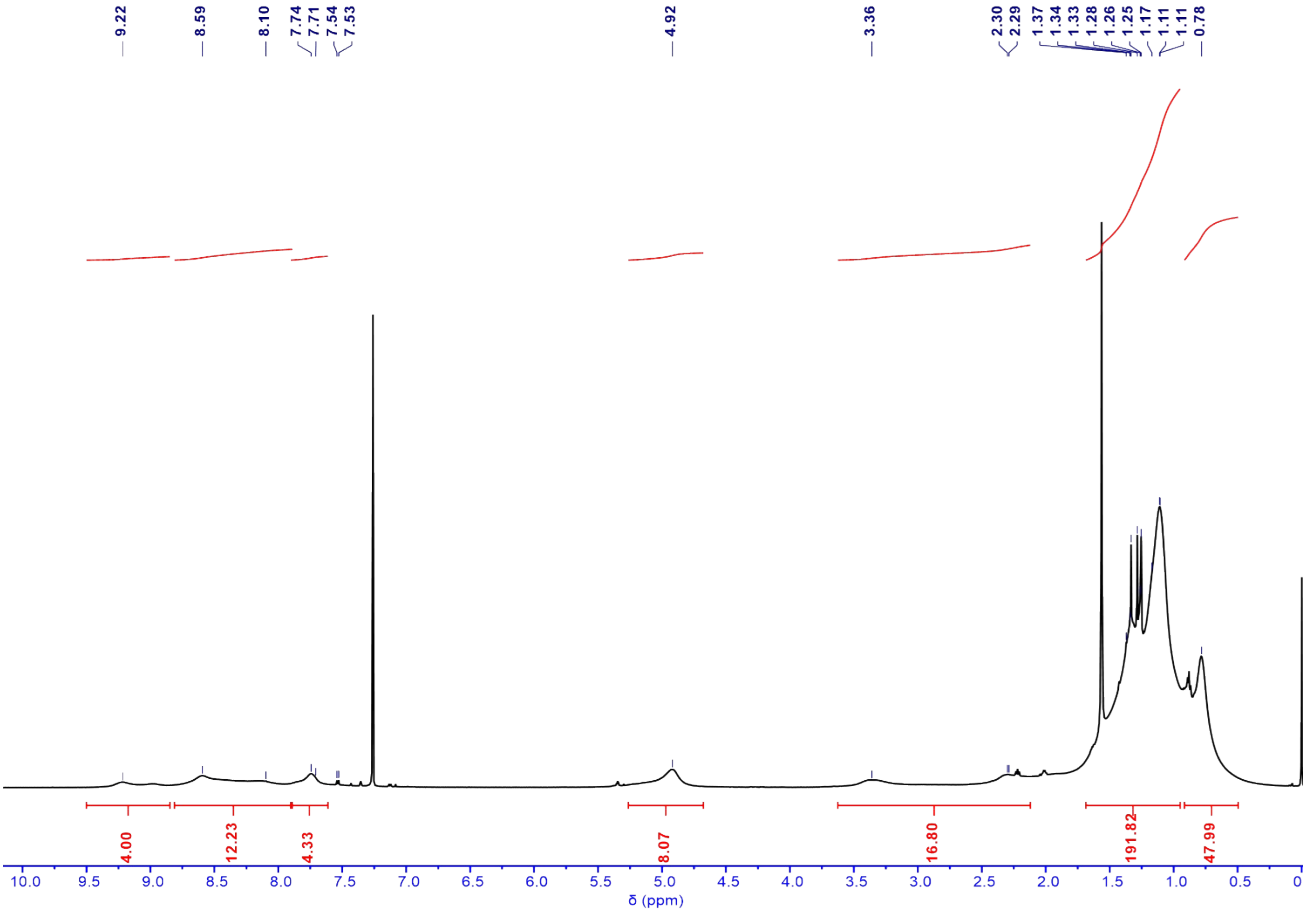

^{1}H-NMR of TBT in $CDCl_3$.

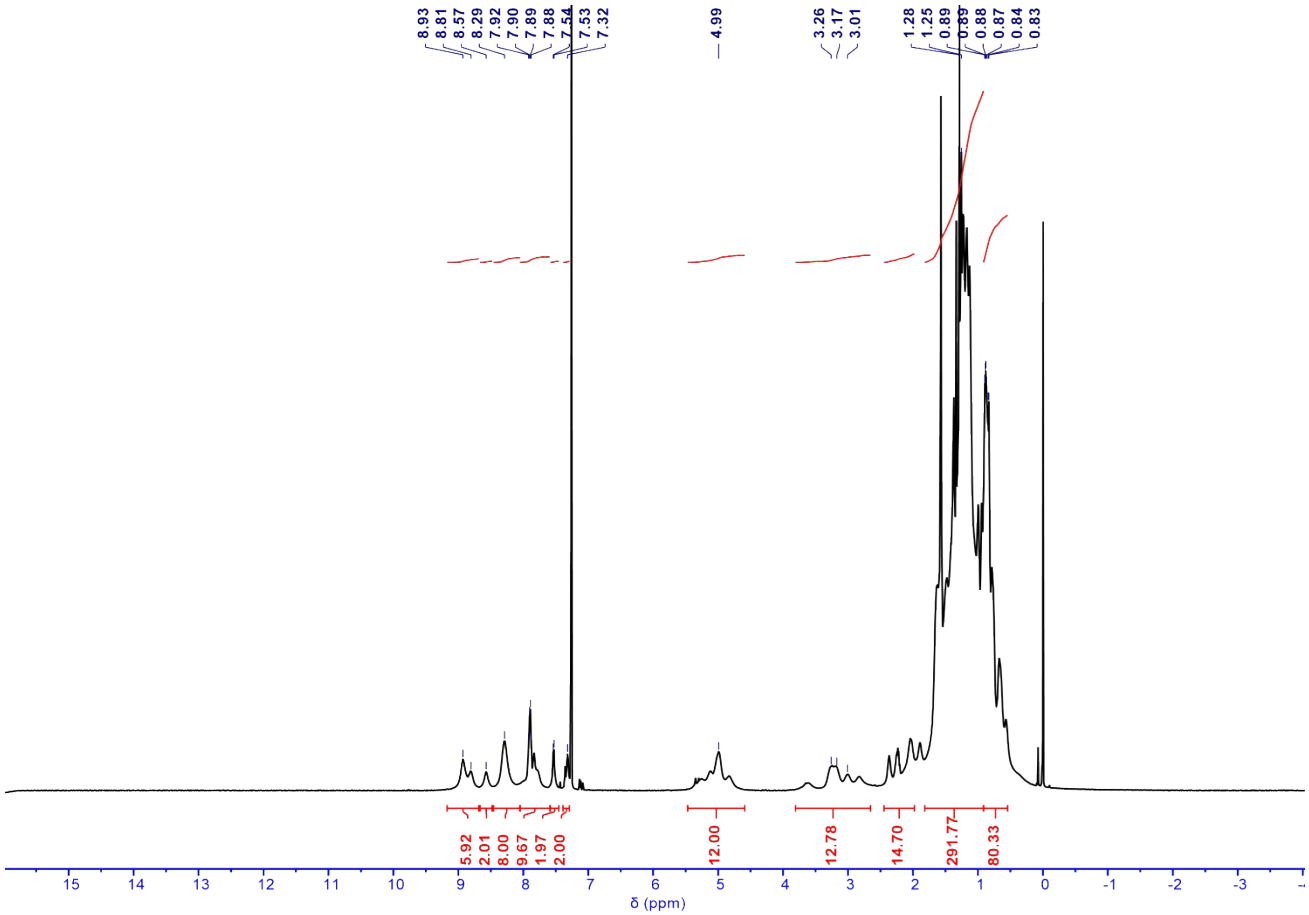

^{1}H-NMR of CH-TRZ in $CDCl_3$.